Pergamon

Geochimica et Cosmochimica Acta, Vol. 61, No. 21, pp. 4571–4582, 1997

0016-7037/97 $17.00 + .00

PII S0016-7037(97)00258-5

Inversion of partial melting through residual peridotites or clinopyroxenes

HAIBO ZOU

Division of Isotope Geochemistry, National High Magnetic Field Laboratory and Department of Geology, Florida State University, Tallahassee, Florida 32306, USA

(*Received October* 7, 1996; *accepted in revised form July* 2, 1997)

Abstract—This paper presents two partial melting inversion methods that permit calculation of the degree of partial melting and source composition for cogenetic melting residues (residual peridotites or clinopyroxenes): the concentration ratio (CR) method and the slope-intercept (SI) method. Neither method requires assumptions regarding source incompatible element concentrations or ratios. The CR method uses variations of between-residue concentration ratios for two incompatible trace elements that have different bulk distribution coefficients to obtain the degrees of partial melting. Source concentrations can be calculated after obtaining the partial melting degree. The SI method employs the slope and the intercept from the $\left[\frac{C_{ra}}{C_{rb}} \text{ vs. } C_{ra} \text{ or } \frac{1}{C_{rb}} \text{ vs. } \frac{1}{C_{ra}}\right]$ diagram to obtain their source concentrations. The degrees of partial melting can be calculated after obtaining the source concentrations. Theoretically, the CR method for residual peridotites or clinopyroxenes may be used for modal and nonmodal batch and nonmodal fractional melting. By comparison, the SI method for residual peridotites can only be applied for modal batch melting while this method for residual clinopyroxenes may be used for both modal and nonmodal batch melting. The CR method and the SI method for residual peridotites are illustrated using the orogenic lherzolites from Lanzo as an example. Results show that both the CR method and the SI method for batch melting can be used for the inversion of partial melting through residues after low degrees of partial melting. *Copyright © 1997 Elsevier Science Ltd*

1. INTRODUCTION

There are two main approaches to investigate the partial melting degree and mantle source composition: inversion through mantle-derived basaltic magmas and inversion through partial melting residues. Inversion of the degree of partial melting and source composition through partial melts has been extensively studied (Treuil and Joron, 1975; Allègre and Minster, 1978; Minster and Allègre, 1978; Hofmann and Feigenson, 1983; Albarède, 1983, 1995; McKenzie and O'Nions, 1991; Maaløe, 1994; Zou and Zindler, 1996; Cebriá and López-Ruiz, 1996; Sims and DePaolo, 1997). In contrast, inversion through melting residues has not been fully carried out.

Conventional methods of trace element modeling of melting residues generally use a direct method of forward calculations to duplicate the observed trace element concentrations in melting residues. The forward calculation has to make assumptions about the source concentrations or the degree of partial melting. One of these two parameters has to be assumed in order to calculate the other. It would be very useful to be able to estimate the degree of partial melting and source concentrations without having to make these assumptions.

The principle aim of this paper is to present two inversion methods to calculate the degree of partial melting and source composition through residual peridotites or clinopyroxenes (cpx). They are the concentration ratio (CR) method and the slope-intercept (SI) method. The CR method uses variations of between-residue concentration ratios for two incompatible trace elements that have different bulk distribution coefficients to obtain the degree of partial melting. Source concentrations can be calculated after obtaining the partial melting degree. The SI method employs the slope and the intercept from the $\frac{C_{ra}}{C_{rb}}$ vs. C_{ra} or $\frac{1}{C_{rb}}$ vs. $\frac{1}{C_{ra}}$ diagram to obtain the source composition. The partial melting degree can be calculated after obtaining the source composition.

There are three main types of partial melting models: batch, fractional, and dynamic melting. The batch melting model assumes that melt remains in equilibrium with the solid throughout the melting event whereas the fractional melting model assumes that (1) melt is removed from the source as it is formed, and (2) only the last drop of melt is in equilibrium with the residue. By definition, residues from fractional melting contain no trapped melt (e.g., Frey et al., 1985). In contrast, dynamic melting involves the retention of a critical fraction of melt in the residue. During dynamic melting, when the melt fraction in the solid matrix is less than the critical value for melt separation, there is no melt extraction (as in batch melting); when the melt fraction in the solid is greater than this critical value, excess melt will be extracted.

In terms of the behavior of bulk partition coefficients (D) during melting processes, there are two modes of melting: modal and nonmodal. If the minerals in the source enter the liquid proportionally to their weight fraction in the source, then the melting is modal; otherwise, it is nonmodal. For modal melting, D does not change ($D = D^0 = P$) during the melting process whereas for nonmodal melting, D varies ($D \neq D^0 \neq P$). Although there is not a unique nonmodal melting model to describe the variation of D during partial melting, the model of Shaw (1970) has been widely accepted and is thus used here. The relationship between D and the

degree of partial melting (f) during nonmodal melting is given by Shaw (1970) as

$$D = \frac{D^0 - Pf}{1-f} \quad (1)$$

D^0 is the bulk distribution coefficients in the initial assemblage, and P is the bulk distribution coefficients of an element for the minerals entering into the liquid (the complete list of symbols is summarized in Appendix).

This paper mainly focuses on the theoretical inversion of modal and nonmodal batch, modal and nonmodal fractional, and modal dynamic melting equations. Extensive case studies will be presented elsewhere.

2. THE CONCENTRATION RATIO METHOD

2.1. Residual Peridotites

2.1.1. Nonmodal batch melting

In the context of nonmodal batch melting, the variation in the concentration of a trace element in a residue, C_r, is given by Shaw (1970) as

$$C_r = \frac{C^0}{(1-f)}\left[\frac{D^0 - Pf}{D^0 + f(1-P)}\right] \quad (2)$$

where C^0 is the concentration in the source. Let the degree of partial melting increase from stage 1 to stage 2 ($f_2 > f_1$). The concentration of a highly incompatible element (e.g., La) in the residue varies from C^1_{ra} to C^2_{ra}, where

$$C^1_{ra} = \frac{C^0_a}{(1-f_1)}\left[\frac{D^0_a - P_a f_1}{D^0_a + f_1(1-P_a)}\right] \quad (3)$$

$$C^2_{ra} = \frac{C^0_a}{(1-f_2)}\left[\frac{D^0_a - P_a f_2}{D^0_a + f_2(1-P_a)}\right] \quad (4)$$

The concentration ratio for the highly incompatible element is given by

$$R_a = \frac{C^1_{ra}}{C^2_{ra}} = \frac{(1-f_2)(D^0_a - P_a f_1)[D^0_a + f_2(1-P_a)]}{(1-f_1)(D^0_a - P_a f_2)[D^0_a + f_1(1-P_a)]} \quad (5)$$

Similarly, the concentration ratio for the less incompatible element is defined by

$$R_b = \frac{C^1_{rb}}{C^2_{rb}} = \frac{(1-f_2)(D^0_b - P_b f_1)[D^0_b + f_2(1-P_b)]}{(1-f_1)(D^0_b - P_b f_2)[D^0_b + f_1(1-P_b)]} \quad (6)$$

Both highly incompatible and not-so-highly incompatible elements are selected because they have large but different concentration ratios in residues formed after different degrees of partial melting. The important feature of R_a and R_b is that both of them are independent of the source concentration (C^0). Equations 5 and 6 constitute a system of nonlinear equations and do not yield analytical solutions. The two unknowns, f_1 and f_2, can be solved by Newton's method for a system of nonlinear equations. After obtaining f_1 and f_2, the source concentrations can be calculated from the relationship

$$C^0 = \frac{C_r(1-f)[D^0 + f(1-P)]}{D^0 - Pf} \quad (7)$$

However, if $D^0_a = P_a$ and $D^0_b = P_b$ in Eqns. 5 and 6, which is the case for modal batch melting, the system yields analytical solutions

$$f_1 = \frac{D^0_a(1-D^0_b)(1-R_a) + D^0_b(1-D^0_a)(R_b-1)}{(R_a-R_b)(1-D^0_a)(1-D^0_b)} \quad (8)$$

$$f_2 = \frac{R_b[D^0_b + f_1(1-D^0_b)] - D^0_b}{1-D^0_b} \quad (9)$$

2.1.2. Nonmodal fractional melting

The concentration of a trace element in the melting residue produced by nonmodal fractional melting is given by Shaw (1970) as

$$C_r = C^0 \frac{1}{1-f}\left(1 - \frac{Pf}{D^0}\right)^{1/P} \quad (10)$$

The concentration ratio for the highly incompatible element is

$$R_a = \frac{C^1_{ra}}{C^2_{ra}} = \frac{1-f_2}{1-f_1}\left(\frac{D^0_a - P_a f_1}{D^0_a - P_a f_2}\right)^{1/P_a} \quad (11)$$

Similarly, for the less incompatible element,

$$R_b = \frac{C^1_{rb}}{C^2_{rb}} = \frac{1-f_2}{1-f_1}\left(\frac{D^0_b - P_b f_1}{D^0_b - P_b f_2}\right)^{1/P_b} \quad (12)$$

After obtaining f_1 and f_2 from the system of Eqns. 11 and 12 by numerical analysis, the source concentrations can be calculated by the following relationship

$$C^0 = C_r(1-f)\left(\frac{D^0}{D^0 - Pf}\right)^{1/P} \quad (13)$$

Note that, if $D^0_a = P_a$ and $D^0_b = P_b$ in Eqns. 11 and 12 (modal fractional melting), the system of equations do not yield any unique solutions for f_1 and f_2 except the following relationship

$$(R_a)^{D^0_a/(1-D^0_a)} = (R_b)^{D^0_b/(1-D^0_b)} = \frac{1-f_1}{1-f_2} \quad (14)$$

Therefore, the concentration ratio (CR) method can not be applied for modal fractional melting.

2.1.3. Dynamic melting

The dynamic melting model was proposed by Langmuir et al. (1977). Only the modal dynamic melting model for melting residues has been formulated till now (McKenzie, 1985a; Albarède, 1995). The concentration of a trace element in the residue of the modal dynamic melting model is given by Albarède (1995) as

$$C_r = C^0(1 - X)^{(1-\phi)(1-D^0)/[(1-\phi)D^0+\phi]} \quad (15)$$

ϕ is threshold value or porosity of the residual solid and is about 1% or less for basaltic melt (McKenzie, 1985b; Qin, 1993); X is the mass fraction of liquid extracted and is related to the degree of partial melting by (Zou and Zindler, 1996)

$$f = X\frac{\rho_s(1-\phi)}{\rho_s(1-\phi)+\rho_f\phi} + \frac{\rho_f\phi}{\rho_s(1-\phi)+\rho_f\phi} \quad (16)$$

where the first and second terms in Eqn. 16 represent the mass fraction of extracted liquid and residual liquid, respectively; P_f is the density of melt (2.8 g/cm^3 for basaltic melts); and P_s is the density of solid matrix (3.3 g/cm^3 for peridotites). The concentration ratio for the highly incompatible element is

$$R_a = \frac{C^1_{ra}}{C^2_{ra}} = \left(\frac{1-X_1}{1-X_2}\right)^{(1-\phi)(1-D^0)/[(1-\phi)D^0_a+\phi]} \quad (17)$$

Similarly, for the less incompatible element,

$$R_b = \frac{C^1_{rb}}{C^2_{rb}} = \left(\frac{1-X_1}{1-X_2}\right)^{(1-\phi)(1-D^0)/[(1-\phi)D^0_b+\phi]} \quad (18)$$

Similar to the case for modal fractional melting, Eqns. 17 and 18 do not yield any unique solutions except the following relationship

$$(R_a)^{[(1-\phi)D^0_a+\phi]/[(1-\phi)(1-D^0_a)]} = (R_b)^{[(1-\phi)D^0_b+\phi]/[(1-\phi)(1-D^0_b)]} = \frac{1-X_1}{1-X_2} \quad (19)$$

Consequently, the CR method can not be applied for modal dynamic melting.

2.2. Residual Clinopyroxenes

If residual peridotites are pervasively serpentinized, they would be unsuitable for inversion of partial melting. In most cases clinopyroxene (cpx) is unaltered, and cpx concentration ratios can be used with confidence in constraining the magmatic processes affecting the rock as a whole. Cpx contains the highest concentrations of incompatible trace elements in typical peridotites (olivine + clinopyroxene + orthopyroxene + spinel) and can be measured in thin sections of serpentinized peridotites using the ion microprobe (Johnson et al., 1990).

Assuming the cpx distribution coefficient is a constant ($D^{0,cpx} = D^{cpx}$), the relationship between $\frac{C_r}{C^0}$ and $\frac{C^{cpx}}{C^{0,cpx}}$ is given by Johnson et al. (1990) as

$$\frac{C_r}{C^0} = \frac{C^{cpx}}{C^{0,cpx}}\frac{D}{D^0} \quad (20)$$

Substitution of Eqn. 20 into Eqns. 2, 10, and 15, respectively, three basic equations describing the variation in concentration of a trace element in cpx of three partial melting models can be obtained as follows:
for nonmodal batch melting,

$$C^{cpx} = C^{0,cpx}\frac{D^0}{D^0+f(1-P)} \quad (21)$$

for nonmodal fractional melting,

$$C^{cpx} = C^{0,cpx}\left(1-\frac{Pf}{D^0}\right)^{(1/P-1)} \quad (22)$$

and for dynamic melting,

$$C^{cpx} = C^{0,cpx}(1-X)^{(1-\phi)(1-D^0)/[(1-\phi)D^0+\phi]} \quad (23)$$

Using the similar way as mentioned in section 2.1., we can obtain a system of equations consisting of the cpx concentration ratio for the highly incompatible element (R_a) and the ratio for the less incompatible element (R_b) from each of the three basic equations (Eqns. 21–23). f_1 and f_2 (or X_1 and X_2) of each model can be obtained by solving the corresponding system of equations consisting of R_a and R_b. The detailed concentration ratios and the solutions for f_1 and f_2 (or X_1 and X_2) for each model are given in Table 1.

After obtaining f or X, the source cpx concentration ($C^{0,cpx}$) for each model can be calculated by substituting f or X into the corresponding one of the three basic equations (Eqns. 21–23). The relationship between the source whole-rock concentration and the source cpx concentration is

$$C^0 = C^{0,cpx}\frac{D^0}{D^{cpx}} \quad (24)$$

3. THE SLOPE-INTERCEPT METHOD

3.1. Residual Whole Rocks

The slope-intercept (SI) method for whole rocks can only be applied for modal batch melting.

3.1.1. Modal batch melting

For elements a (highly incompatible) and b (not-so-highly incompatible), their concentrations in the residue during modal batch melting, C_{ra} and C_{rb}, respectively, are given by

$$C_{ra} = \frac{D^0_aC^0_a}{D^0_a+f(1-D^0_a)} \quad (25)$$

$$C_{rb} = \frac{D^0_bC^0_b}{D^0_b+f(1-D^0_b)} \quad (26)$$

The relationship between C_{ra}/C_{rb} and C_{ra} can be derived from Eqns. 25 and 26 as follows:

$$\frac{C_{ra}}{C_{rb}} = \left[D^0_b - \frac{D^0_a(1-D^0_b)}{1-D^0_a}\right]\frac{C_{ra}}{D^0_bC^0_b} + \frac{D^0_a(1-D^0_b)C^0_a}{D^0_b(1-D^0_a)C^0_b} \quad (27)$$

Equation 27 shows that the ratio $\frac{C_{ra}}{C_{rb}}$ is a linear function of the concentration C_{ra}. The slope (S) and intercept (I) of the straight line described by Eqn. 27 can be expressed as

$$S = \left[D^0_b - \frac{D^0_a(1-D^0_b)}{1-D^0_a}\right]\frac{1}{D^0_bC^0_b} \quad (28)$$

$$I = \frac{D^0_a(1-D^0_b)C^0_a}{D^0_b(1-D^0_a)C^0_b} \quad (29)$$

Table 1. Summary of the concentration ratio method.

Model	C_r	R_a	R_b	f_1	f_2
Whole rock					
Modal batch	$\frac{D^0C^0}{D^0+f(1-D^0)}$	$\frac{D_a^0+f_2(1-D_a^0)}{D_a^0+f_1(1-D_a^0)}$	$\frac{D_b^0+f_2(1-D_b^0)}{D_b^0+f_1(1-D_b^0)}$	$\frac{D_a^0(1-D_b^0)(1-R_a)+D_b^0(1-D_a^0)(R_b-1)}{(1-D_a^0)(1-D_b^0)(R_a-R_b)}$	$\frac{R_b[D_b^0+f_1(1-D_b^0)]-D_b^0}{1-D_b^0}$
Non-modal batch	$\frac{C^0}{(1-f)}\left[\frac{D^0-Pf}{D^0+f(1-P)}\right]$	$\frac{(1-f_2)(D_a^0-P_af_1)[D_a^0+f_2(1-P_a)]}{(1-f_1)(D_a^0-P_af_2)[D_a^0+f_1(1-P_a)]}$	$\frac{(1-f_2)(D_b^0-P_bf_1)[D_b^0+f_2(1-P_b)]}{(1-f_1)(D_b^0-P_bf_2)[D_b^0+f_1(1-P_b)]}$	Numerical solution	
Modal fractional	$C^0(1-f)^{(1/D^0-1)}$	$\left(\frac{1-f_1}{1-f_2}\right)^{(1/D_a^0-1)}$	$\left(\frac{1-f_1}{1-f_2}\right)^{(1/D_b^0-1)}$	Not applicable	
Non-modal fractional	$C^0\frac{1}{1-f}\left(1-\frac{Pf}{D^0}\right)^{1/P}$	$\frac{1-f_2}{1-f_1}\left(\frac{D_a^0-P_af_1}{D_a^0-P_af_2}\right)^{1/P_a}$	$\frac{1-f_2}{1-f_1}\left(\frac{D_b^0-P_bf_1}{D_b^0-P_bf_2}\right)^{1/P_b}$	Numerical solution	
Dynamic	$C^0(1-X)^{(1-\phi)(1-D^0)/[(1-\phi)D^0+\phi]}$	$\left(\frac{1-X_1}{1-X_2}\right)^{(1-\phi)(1-D_a^0)/[(1-\phi)D_a^0+\phi]}$	$\left(\frac{1-X_1}{(1-X_2}\right)^{(1-\phi)(1-D_b^0)/[(1-\phi)D_b^0+\phi]}$	Not applicable	
CPX					
Modal batch	$C^{0,cpx}\frac{D^0}{D^0+f(1-D^0)}$	$\frac{D_a^0+f_2(1-D_a^0)}{D_a^0+f_1(1-D_a^0)}$	$\frac{D_b^0+f_2(1-D_b^0)}{D_b^0+f_1(1-D_b^0)}$	$\frac{D_a^0(1-D_b^0)(1-R_a)+D_b^0(1-D_a^0)(R_b-1)}{(1-D_a^0)(1-D_b^0)(R_a-R_b)}$	$\frac{R_b[D_b^0+f_1(1-D_b^0)]-D_b^0}{1-D_b^0}$
Non-modal batch	$C^{0,cpx}\frac{D^0}{D^0+f(1-P)}$	$\frac{D_a^0+f_2(1-P_a)}{D_a^0+f_1(1-P_a)}$	$\frac{D_b^0+f_2(1-P_b)}{D_b^0+f_1(1-P_b)}$	$\frac{D_a^0(1-P_a)(1-R_a)+D_b^0(1-P_a)(R_b-1)}{(1-P_a)(1-P_b)(R_a-R_b)}$	$\frac{R_b[D_b^0+f_1(1-P_b)]-D_b^0}{1-P_b}$
Modal fractional	$C^{0,cpx}(1-f)^{(1/D^0-1)}$	$\left(\frac{1-f_1}{1-f_2}\right)^{(1/D_a^0-1)}$	$\left(\frac{1-f_1}{1-f_2}\right)^{(1/D_b^0-1)}$	Not applicable	
Non-modal fractional	$C^{0,cpx}\left(1-\frac{Pf}{D^0}\right)^{(1/P-1)}$	$\left(\frac{D_a^0-P_af_1}{D_a^0-P_af_2}\right)^{(1/P_a-1)}$	$\left(\frac{D_b^0-P_bf_1}{D_b^0-P_bf_2}\right)^{(1/P_b-1)}$	$\frac{D_a^0-Q_a(D_a^0-P_af_2)}{P_a}$	$\frac{P_bD_a^0(1-Q_a)+P_aD_b^0(Q_b-1)}{P_aP_b(Q_b-Q_a)}$
Dynamic	$C^{0,cpx}(1-X)^{(1-\phi)(1-D^0)/[(1-\phi)D^0+\phi]}$	$\left(\frac{1-X_1}{1-X_2}\right)^{(1-\phi)(1-D_a^0)/[(1-\phi)D_a^0+\phi]}$	$\left(\frac{1-X_1}{1-X_2}\right)^{(1-\phi)(1-D_b^0)/[(1-\phi)D_b^0+\phi]}$	Not applicable	

We can obtain S and I from the $\frac{C_{ra}}{C_{rb}}$ vs. C_{ra} diagram if there is a significant linear relationship between $\frac{C_{ra}}{C_{rb}}$ and C_{ra} for a set of peridotites. Source concentrations can be calculated by

$$C_a^0 = \frac{I}{S}\left[\frac{D_b^0(1-D_a^0)}{D_a^0(1-D_b^0)} - 1\right] \tag{30}$$

$$C_b^0 = \frac{C_a^0}{SC_a^0 + I} \tag{31}$$

A linear relationship between $\frac{1}{C_{ra}}$ and $\frac{1}{C_{rb}}$ for modal batch melting can also be obtained from Eqns. 25 and 26 as follows:

$$\frac{1}{C_{rb}} = S\frac{I}{C_{ra}} + I \tag{32}$$

where the slope (S) and the intercept (I) of the straight line described by Eqn. 32 can be expressed as

$$S = \frac{D_a^0(1-D_b^0)C_a^0}{D_b^0(1-D_a^0)C_b^0} \tag{33}$$

$$I = \left[D_b^0 - \frac{D_a^0(1-D_b^0)}{1-D_a^0}\right]\frac{1}{D_b^0 C_b^0} \tag{34}$$

After obtaining S and I in the $\frac{1}{C_{rb}}$ vs. $\frac{1}{C_{ra}}$ diagram, source concentrations are given in Table 2.

3.2. Residual Clinopyroxenes

In contrast to the case for whole rocks, the SI method for residual clinopyroxenes can be applied to nonmodal batch melting.

3.2.1. Nonmodal batch melting

The basic equation for the variation of a trace element in cpx during nonmodal batch melting has been given in Eqn. 21. Similarly, we can obtain the following two linear relationships:

$$\frac{C_a^{cpx}}{C_b^{cpx}} = \left[D_b^0 - \frac{D_a^0(1-P_b)}{1-P_a}\right]\frac{C_a^{cpx}}{D_b^0 C_b^{0,cpx}} + \frac{D_a^0(1-P_b)C_a^{0,cpx}}{D_b^0(1-P_a)C_b^{0,cpx}} \tag{35}$$

$$\frac{1}{C_b^{cpx}} = \frac{D_a^0(1-P_b)C_a^{0,cpx}}{D_b^0(1-P_a)C_b^{0,cpx}}\frac{1}{C_a^{cpx}} + \left[D_b^0 - \frac{D_a^0(1-P_b)}{1-P_a}\right]\frac{1}{D_b^0 C_b^{0,cpx}} \tag{36}$$

Their slope, intercept, and source cpx concentrations are also given in Table 2.

4. AN APPLICATION

Ultramafic rocks of mantle origin have three principle modes of occurrence at the earth's surface: (1) the lower portions of some ophiolite complex, typically comprising high-sheared harzburgites; (2) discrete nodules of peridotites which are brought to the surface by alkalic volcanoes and kimberlites; and (3) large orogenic peridotites (also called alpine peridotites or high-temperature peridotites), ranging from tens of square meters to hundreds of square kilometers in extent, which have been tectonically emplaced into the crust (e.g., Zindler et al., 1983). Ophiolite harzburgites are produced by high degree of partial melting, and they have extremely low concentrations of incompatible trace elements. Inversion through ophiolite harzburgites thus requires very accurate measurement of their extremely low concentrations. Peridotite nodules often have complex geochemical characteristics attributed to mantle metasomatism (e.g., Zindler et al., 1983; Kempton, 1985; Menzies et al., 1985). Much of the compositional complexity found in peridotite nodules has been attributed to interactions within the mantle of peridotites with fluids which culminated in the alkalic volcanism which transport the mantle samples to the crust (e.g., Frey, 1984; Menzies et al., 1985). The abundant evidence for metasomatism in peridotite nodules reflects localized metasomatic effects caused by nearby igneous intrusions, perhaps associated with the volcanism that sampled the peridotite nodules (Wilshire, 1984). Therefore, only the peridotite nodules free of metasomatism are suitable for inversion of the degree of partial melting and source composition. Large orogenic peridotite bodies are geochemically simple and are emplaced into the crust by processes unrelated to volcanism. Because they do not suffer from the context and scale problems inherent in nodules, nor do they display the nearly total depletion in large-ion-lithophile elements observed in ophiolite harzburgites (Zindler et al., 1983; Prinzhofer and Allègre, 1985), they are perhaps the most suitable for geochemical inversion of partial melting through whole-rock residues.

The minimum requirements for meaningful inversion is that (1) the samples being inverted can be argued to be residues after melting a common, homogeneous source, and (2) the data must be of high quality. For the CR method, the following requirement must also be satisfied

$$R_{La} > R_{Nd} > R_{Sm} > \cdots\cdots > R_{Lu} \tag{37}$$

For the SI method, a suite of data must show a significant linear relationship.

4.1. Application to Orogenic Lherzolites from Lanzo

The application of the CR method and the SI method can be demonstrated using trace element data for orogenic lherzolites from Lanzo, Italian Alps. The orogenic lherzolites from Lanzo display a wide range of variations in light rare earth elements (LREE) and a relatively small range of variations for the heavy rare earth elements (HREE), a feature resulting from partial melting of an originally homogeneous lherzolitic upper mantle. These lherzolites are considered as residues after extraction of basaltic melt (Loubet and

Table 2. Summary of the slope-intercept method.

Batch melting	C_r	Plot	Slope	Intercept	C_a^0 for whole rock or $C_a^{0,cpx}$ for cpx	C_b^0 for whole rock or $C_b^{0,cpx}$ for cpx
Whole rock						
Modal	$\frac{D^0C^0}{D^0+f(1-D^0)}$	$\frac{C_{ra}}{C_{rb}}$ vs. C_{ra}	$\left[D_b^0-\frac{D_a^0(1-D_b^0)}{1-D_a^0}\right]\frac{1}{D_b^0C_b^0}$	$\frac{D_a^0(1-D_b^0)C_a^0}{D_b^0(1-D_a^0)C_b^0}$	$\frac{I}{S}\left[\frac{D_b^0(1-D_a^0)}{D_a^0(1-D_b^0)}-1\right]$	$\frac{C_a^0}{SC_a^0+I}$
		$\frac{1}{C_{rb}}$ vs. $\frac{1}{C_{ra}}$	$\frac{D_a^0(1-D_b^0)C_a^0}{D_b^0(1-D_a^0)C_b^0}$	$\left[D_b^0-\frac{D_a^0(1-D_b^0)}{1-D_a^0}\right]\frac{1}{D_b^0C_b^0}$	$\frac{S}{I}\left[\frac{D_b^0(1-D_a^0)}{D_a^0(1-D_b^0)}-1\right]$	$\frac{C_a^0}{IC_a^0+S}$
Non-modal	$\frac{C^0}{(1-f)}\frac{D^0-Pf}{D^0+f(1-P)}$	$\frac{C_{ra}}{C_{rb}}$ vs. C_{ra}		Not applicable		
		$\frac{1}{C_{rb}}$ vs. $\frac{1}{C_{ra}}$		Not applicable		
CPX						
Modal	$C^{0,cpx}\frac{D^0}{D^0+f(1-D^0)}$	$\frac{C_{ra}}{C_{rb}}$ vs. C_{ra}	$\left[D_b^0-\frac{D_a^0(1-D_b^0)}{1-D_a^0}\right]\frac{1}{D_b^0C_b^{0,cpx}}$	$\frac{D_a^0(1-D_b^0)C_a^{0,cpx}}{D_b^0(1-D_a^0)C_b^{0,cpx}}$	$\frac{I}{S}\left[\frac{D_b^0(1-D_a^0)}{D_a^0(1-D_b^0)}-1\right]$	$\frac{C_a^{0,cpx}}{SC_a^{0,cpx}+I}$
		$\frac{1}{C_{rb}}$ vs. $\frac{1}{C_{ra}}$	$\frac{D_a^0(1-D_b^0)C_a^{0,cpx}}{D_b^0(1-D_a^0)C_b^{0,cpx}}$	$\left[D_b^0-\frac{D_a^0(1-D_b^0)}{1-D_a^0}\right]\frac{1}{D_b^0C_b^{0,cpx}}$	$\frac{S}{I}\left[\frac{D_b^0(1-D_a^0)}{D_a^0(1-D_b^0)}-1\right]$	$\frac{C_a^{0,cpx}}{IC_a^{0,cpx}+S}$
Non-modal	$C^{0,cpx}\frac{D^0}{D^0+f(1-P)}$	$\frac{C_{ra}}{C_{rb}}$ vs. C_{ra}	$\left[D_b^0-\frac{D_a^0(1-P_b)}{1-P_a}\right]\frac{1}{D_b^0C_b^{0,cpx}}$	$\frac{D_a^0(1-P_b)C_a^{0,cpx}}{D_b^0(1-P_a)C_b^{0,cpx}}$	$\frac{I}{S}\left[\frac{D_b^0(1-P_a)}{D_a^0(1-P_b)}-1\right]$	$\frac{C_a^{0,cpx}}{SC_a^{0,cpx}+I}$
		$\frac{1}{C_{rb}}$ vs. $\frac{1}{C_{ra}}$	$\frac{D_a^0(1-P_b)C_a^{0,cpx}}{D_b^0(1-P_a)C_b^{0,cpx}}$	$\left[D_b^0-\frac{D_a^0(1-P_b)}{1-P_a}\right]\frac{1}{D_b^0C_b^{0,cpx}}$	$\frac{S}{I}\left[\frac{D_b^0(1-P_a)}{D_a^0(1-P_b)}-1\right]$	$\frac{C_a^{0,cpx}}{IC_a^{0,cpx}+S}$

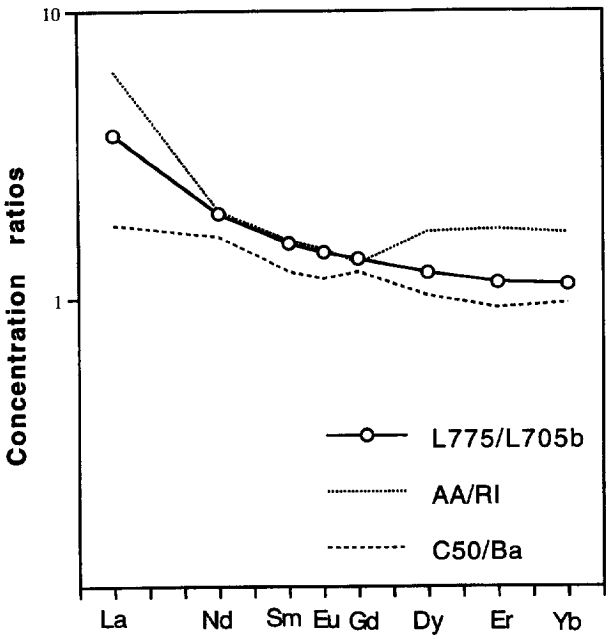

Fig. 1. Concentration ratios of different pairs of samples. L775, L705b, AA, RI, C50, and Ba are sample names.

Allègre, 1982). Trace element concentrations are from Loubet and Allègre (1982) and were measured by isotope dilution mass spectrometry with an accuracy of better than 2.5%. Samples L775 and L705b are selected for inversion using the CR method because they are the only pairs that completely satisfy the requirements for the CR method (e.g., inequality 37; Fig. 1). Data and results of the CR method are summarized in Table 3. The relevant parameters are given in the notation of Table 3. R_a is taken as the La concentration ratio (L775/L705b), and the Nd concentration ratio is used as R_b:

$$R_a = R_{La} = 0.067/0.018 = 3.72 \quad (38)$$

$$R_b = R_{Nd} = 0.537/0.271 = 1.98 \quad (39)$$

Substitution of these concentration ratios into Eqns. 8 and 9 for modal batch melting, we obtain $f_1 = 0.39\%$ and $f_2 = 2.41\%$. Similarly, using La concentration ratio as R_a but using Sm, Eu, or Gd concentration ratio as R_b, we can get three additional sets of f_1 and f_2 values. Averaging the values obtained for the four rare earth elements (Nd, Sm, Eu, Gd) yields $\overline{f_1} = 0.39\%$ and $\overline{f_2} = 2.41\%$ (Table 3). Using these obtained values for $\overline{f_1}$ or $\overline{f_2}$ and the trace element concentrations in L775 or L705b, Eqn. 7 allows us to calculate all the REE source concentrations for modal batch melting by setting $P = D^0$ (Table 3 and Fig. 2).

Using the same concentration ratios but solving the system of Eqns. 5 and 6 for nonmodal batch melting, we obtain partial melting degrees of 0.38% for L775 and 2.24% for L705b (these melting degrees represent averages for calculations made with R_bs for four different REEs, ranging from Nd to Gd; Table 3), which is very similar to those for modal batch melting. The REE source concentrations for nonmodal batch melting can be calculated directly from Eqn. 7.

Considering L705b has the lowest La concentrations among the samples of the Lanzo lherzolites, its degree of partial melting (2.41%) suggests that the Lanzo lherzolites are residues after extraction of a small percent of basaltic melt (<3%). This is consistent with previous studies (Loubet et al., 1975; Loubet and Allègre, 1982).

As mentioned in section 2.1.2. and 2.1.3., the CR method can not be used for modal fractional melting or modal dynamic melting. Theoretically, the CR method may be applied for nonmodal fractional melting. However, when applying this method for nonmodal fractional melting to the Lanzo lherzolites, the system of Eqns. 11 and 12 seldom yields meaningful solutions in part because the solutions are very sensitive to the extent to which P is close to D^0 (recall that if $P = D^0$, the system of Eqns. 11 and 12 becomes that for modal fractional melting). Therefore, no inversion results from the CR method for modal or nonmodal fractional melting or modal dynamic melting are listed in Table 3.

Since the SI method uses the slope and the intercept from a set of data instead of using two concentration ratios directly, the requirement of concentration data for the SI method is less strict than that for the CR method. The inversion results using the SI method for the Lanzo peridotites are shown in Fig. 3 and are summarized in Table 4. Because both C_{ra} and C_{rb} are low for peridotites and small measurement uncertainty in C_{ra} or C_{rb} will produce large variations in $\frac{1}{C_{ra}}$ or $\frac{1}{C_{rb}}$, we have used the $\frac{C_{ra}}{C_{rb}}$ vs. C_{ra} diagram instead of the $\frac{1}{C_{rb}}$ vs. $\frac{1}{C_{ra}}$ diagram. The La-La/REE diagrams (except the La-La/Ce diagram) show significant linear trends, which might indicate that batch melting equations can provide a good description for these residues after low degrees of partial melting. The calculated source La concentration from La-La/Nd, La-La/Sm, La-La/Eu, and La-La/Gd diagrams for the Lanzo lherzolites are 0.219, 0.207, 0.243, and 0.239 ppm, respectively. The average value $\overline{C^0_{La}}$ is, therefore, 0.227 ppm. Using $\overline{C^0_{La}} = 0.227$ ppm and the slope and the intercept from each La-La/REE diagram, we can calculate source concentrations for other REEs (Table 4). The calculated source concentrations from the SI method are similar to those from the CR method (Fig. 4).

We have used the batch melting equations to estimate the source compositions for the Lanzo lherzolites by both the CR method and the SI method. Since the type of melting must be batch melting until the source becomes permeable (e.g., Maaløe, 1994), the source trace element concentrations estimated from batch melting equations are likely to be reliable at low degrees of partial melting (Maaløe, 1994; Zou and Zindler, 1996). Calculations have shown that the Lanzo lherzolites are indeed the residues after low degrees of partial melting.

In summary, the CR method has three steps: (1) to judge if inequality 37 is satisfied, (2) to calculate the values of $\overline{f_1}$ and $\overline{f_2}$, and (3) to calculate the source concentrations for all REEs using $\overline{f_1}$ or $\overline{f_2}$. The SI method also constitutes three steps: (1) to judge if a set of data satisfy a linear relationship in the La-La/REE diagrams, (2) to calculate the average source La concentration $\overline{C^0_{La}}$, and (3) to calculate the source

Table 3. Estimation of partial melting degrees and mantle source compositions from the Lanzo peridotites using the CR method.

						Modal batch						Non-modal batch					
	D^0	P	L775 C_1 (ppm)	L705b C_2 (ppm)	R	f_1 (%)	f_2 (%)	C^0 (ppm)	$(C^0)_N$	$\overline{C^0}$ (ppm)	$(\overline{C^0})_N$	f_1 (%)	f_2 (%)	C^0 (ppm)	$(C^0)_N$	$\overline{C^0}$ (ppm)	$(\overline{C^0})_N$
La	0.0035	0.0115	0.067	0.018	3.72					0.141	0.60					0.140	0.59
Nd	0.0164	0.0578	0.537	0.271	1.98	0.39	2.41	0.663	1.45	0.663	1.45	0.38	2.25	0.657	1.44	0.657	1.44
Sm	0.0308	0.1144	0.225	0.144	1.56	0.38	2.37	0.253	1.70	0.252	1.70	0.37	2.21	0.251	1.68	0.252	1.69
Eu	0.0391	0.1485	0.0954	0.0656	1.45	0.39	2.39	0.105	1.88	0.105	1.88	0.37	2.21	0.104	1.86	0.104	1.86
Gd	0.0478	0.1848	0.375	0.271	1.38	0.41	2.47	0.401	2.04	0.404	2.05	0.39	2.28	0.404	2.05	0.404	2.05
Dy	0.0984	0.4104	0.492	0.398	1.24					0.509	2.08					0.509	2.08
Er	0.2396	1.0426	0.309	0.270	1.14					0.313	1.96					0.313	1.96
Yb	0.4379	1.9286	0.327	0.29	1.13					0.329	2.07					0.330	2.08
$\bar{f}$						0.39	2.41					0.38	2.24				

Trace element data are from Loubet and Allègre (1982). D^0 = source bulk distribution coefficient; P = bulk distribution coefficient for the minerals entering into the liquid. Average P values from Eqn. B7 of Maaløe (1994) are used here. C^0 is the calculated source concentrations using f_1 and C_1 (or f_2 and C_2). $(C^0)_N$ is the chondrite-normalized C^0 value; $\bar{f}$ is the average values of calculated partial melting degrees; $\overline{C^0}$ is the calculated source concentrations using $\bar{f}$; $(\overline{C^0})_N$ is the chondrite-normalized $\overline{C^0}$. The REE distribution coefficients of set 1 by Frey et al. (1978) are used in the calculations. The mineral proportions are from Johnson et al. (1990) as: 55% olivine, 20% opx, 15% cpx, and 10% garnet. The mineral proportion of Maaløe and Aoki (1977) and Maaløe (1994) (66% olivine, 20% opx, 8% cpx, and 6% garnet) is suitable for depleted mantle source (e.g., MORB source) instead of primitive mantle source and therefore is not used for the inversion of the lherzolites from Lanzo. The distribution coefficients of Gd, Dy and Er are not listed in Frey et al. (1978) and their D^0 and P values are thus calculated by interpolation: $D^0_{Gd} = (D^0_{Eu} + D^0_{Tb})/2$, $P_{Gd} = (P_{Eu} + P_{Tb})/2$, $D^0_{Dy} = (D^0_{Tb} + D^0_{Ho})/2$, $P_{Dy} = (P_{Tb} + P_{Ho})/2$, $D^0_{Er} = (2D^0_{Ho} + D^0_{Yb})/3$, and $P_{Er} = (2P_{Ho} + P_{Yb})/3$, where $D^0_{Tb} = 0.0564$, $P_{Tb} = 0.2211$, $D^0_{Ho} = 0.1404$, and $P_{Ho} = 0.5996$. R = concentration ratio = concentration in L775/concentration in L705b; La concentration ratio is used as R_a (the concentration ratio for the highly incompatible element) and the concentration ratio for other REE as R_b (the concentration ratio for the less incompatible element). f_1 = partial melting degree for L775; f_2 = partial melting degree for L705b; Only LREEs (instead of HREEs) are used to calculate the partial melting degree because (1) the bulk distribution coefficients of LREEs are insensitive to mineral proportions (e.g., garnet content), and (2) variations in LREE concentrations in residues are sensitive to variations of partial melting degrees. Ce is not used to calculate the degree of partial melting because Ce can be readily affected by alterations (e.g., Ottonello, et al., 1979); REE abundances for C1 chondrites are from Anders and Ebihara (1982).

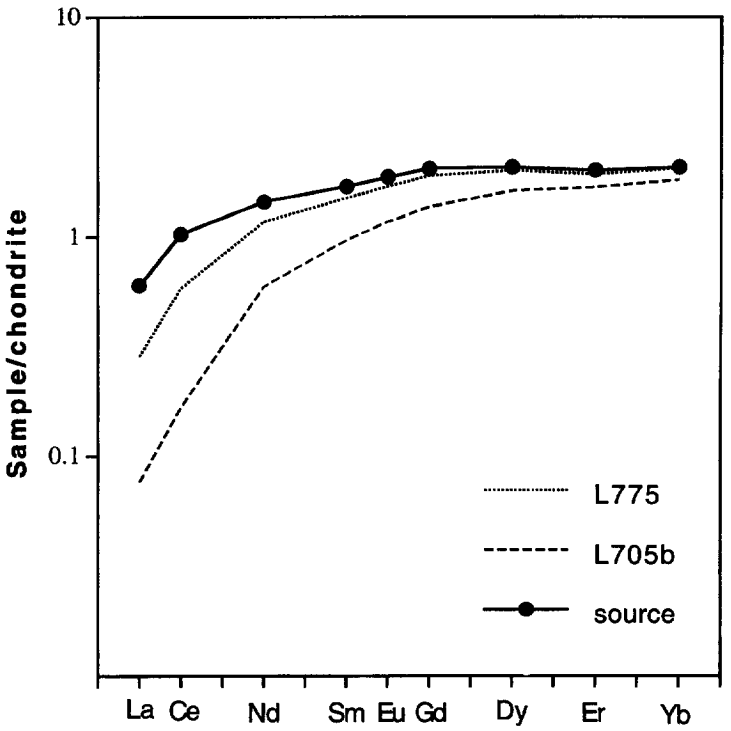

Fig. 2. C1 chondrite-normalized source REE compositions for samples L775 and L705b using the CR method. REE abundances for C1 chondrites are from Anders and Ebihara (1982). The $(\overline{C^0_{Ce}})_N$ is estimated as the average value of $(\overline{C^0_{La}})_N$ and $(\overline{C^0_{Nd}})_N$.

concentrations for other REEs using $\overline{C^0_{La}}$. The key for the CR method is to calculate fairly accurate $\overline{f_1}$ and $\overline{f_2}$ while the key for the SI method is to obtain a fairly accurate $\overline{C^0_{La}}$.

5. DISCUSSION AND CONCLUSIONS

The composition of partial melts may be affected by fractional crystallization and the shape of melting region (O'Hara, 1985; Maaløe and Johnson, 1986; Plank and Langmuir, 1992; Maaløe, 1996). Inversion through melting residues is not affected by these parameters but requires accurate measurement of low concentrations of incompatible trace elements. If the melting residues are modified by metasomatism after partial melting, the inversion methods presented here are not applicable. It is not very likely to obtain fairly accurate concentrations of residues before metasomatism through correction of metasomatized residues, therefore, it is important to find the right samples for reliable inversion. Figures 1–3 can be used to identify these right samples.

Most previous approaches for estimating the composition of the primordial mantle were based on a comparison with primitive meteorites and fertile peridotites (e.g., Ringwood, 1975; Jagoutz et al., 1979; Sun, 1982; Zindler and Hart, 1986). The estimates of volatile and siderophilic elements may be poor in the estimates because of the different thermal histories of the Earth and the meteorite parent bodies and the fact that the Earth material was fractionated into core, mantle, and crust (Hartmann and Wedepohl, 1993). In a pioneering paper, Jagoutz et al. (1979) used nearly-primitive peridotite xenoliths to estimate element abundances in the primitive mantle, for example, the REE contents of the Earth's mantle of Jagoutz et al. (1979) are calculated by multiplying REE/Sc ratios in C1 chondrites by Sc content of the Earth's mantle which is estimated by averaging measured Sc contents in six nearly-primitive ultramafic nodules. This approach assumes that the Earth's primitive mantle and C1 chondrites have similar ratios of refractory (nonvolatile) elements. Because of the limited size, data on such xenoliths should be supplemented by investigations of fertile orogenic peridotites. Hartmann and Wedepohl (1993) used fertile orogenic peridotites from Balmuccia and Baldissero to approach element abundance in the primitive mantle. Their estimates are calculated from 97.2% Balmuccia lherzolites + 2.8% bulk crust. The above two approaches can yield good estimates for major elements and compatible trace elements. They might not be the most suitable for incompatible elements because (1) unlike the case for compatible trace elements and major elements, the concentrations and concentration ratios of incompatible trace elements in melting residues are sensitive to low degrees of partial melting, and (2) there are large uncertainties in the estimated concentrations of trace elements of the bulk crust (Taylor and McLennan, 1985; Wedepohl, 1991) and our knowledge of the lower crust is limited. It is believed that, along with the improvement of our knowledge of distribution coefficients, application of the inversion methods through residual peridotite xenoliths and fertile peridotites worldwide has the potential to provide a good estimate of the concentrations of incompatible trace elements in the primitive mantle.

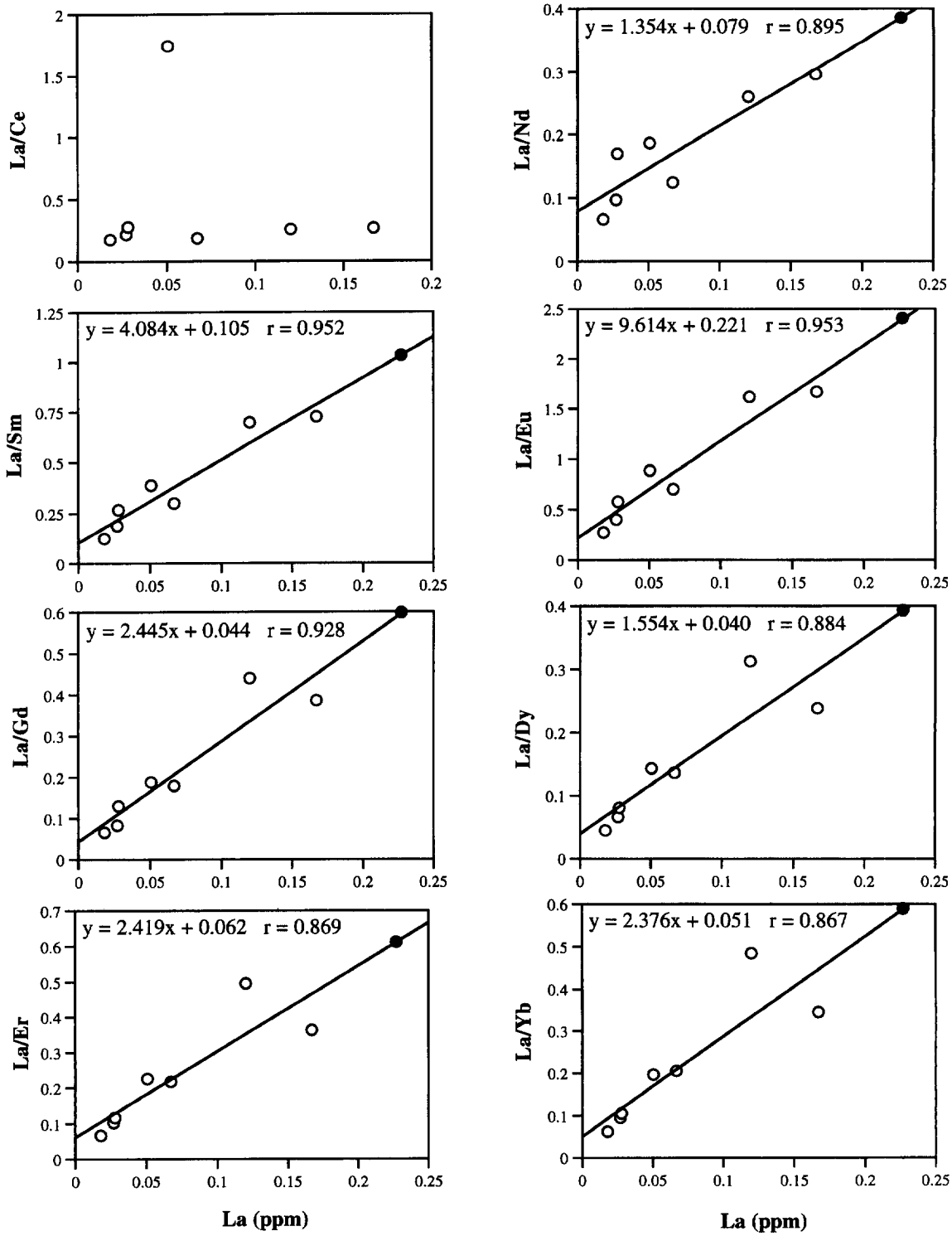

Fig. 3. La-La/REE diagrams to obtain the slope and the intercept for the SI method. The La-La/REE diagrams (except the La-La/Ce diagram) show statistically significant linear relationship (unlike other REEs, Ce can be readily affected by alterations). Open circles represent sample compositions, and filled circles represent the calculated source composition from the SI method. r is the correlation coefficient.

This paper investigates the theoretical inversion of modal and nonmodal batch, modal and nonmodal fractional, and modal dynamic melting equations for cogenetic melting residues (residual peridotites or clinopyroxenes) using the CR method and the SI method. The details of the CR method and the SI method are summarized in Tables 1 and 2, respec-

Table 4. Estimation of mantle source compositions from the Lanzo peridotites using the SI method.

Figures	La-La/Ce	La-La/Nd	La-La/Sm	La-La/Eu	La-La/Gd	La-La/Dy	La-La/Er	La-La/Yb
S (slope)	na	1.354	4.084	9.614	2.445	1.554	2.419	2.376
I (intercept)	na	0.079	0.105	0.221	0.044	0.040	0.062	0.051
r	na	0.895	0.952	0.953	0.928	0.884	0.869	0.867
C^0_{La}	na	0.219	0.207	0.243	0.239	—	—	—
C^0_b	na	0.583	0.218	0.095	0.381	—	—	—
$\overline{C^0_{La}}$	na	0.227	0.227	0.227	0.227	0.227	0.227	0.227
$\overline{C^0_b}$	na	0.588	0.220	0.094	0.379	0.578	0.371	0.385
$\overline{C^0_{La}}/\overline{C^0_b}$	na	0.386	1.032	2.415	0.599	0.393	0.612	0.590

Source La concentration is obtained by $C^0_{La} = \frac{I}{S}\left[\frac{D^0_b(1 - D^0_{La})}{D^0_{La}(1 - D^0_b)} - 1\right]$; Source compositions for rare earth elements other than La are calculated by $C^0_b = C^0_{La}/(SC^0_{La} + I)$; only four calculated C^0_{La} values from La-La/Nd, La-La/Sm, La-La/Eu, and La-La/Gd diagrams are listed in Table 4 because (1) a set of data do not show a significant linear trend in the La/Ce vs. La diagram (unlike other REEs, Ce can be readily affected by alterations) and (2) in contrast to the cases for the four La-La/LREE diagrams, the calculated C^0_{La} values from La-La/Dy, La-La/Er, and La-La/Yb diagrams are very sensitive to the uncertainties of the mineral proportions (the distribution coefficients of HREEs, such as Dy, Er and Yb, are sensitive to the source garnet content). $\overline{C^0_{La}}$ is the average value of source La concentrations (C^0_{La}) obtained from the four La-La/LREE diagrams; $\overline{C^0_b}$ is the source compositions for rare earth elements other than La and $\overline{C^0_b} = \overline{C^0_{La}}/(S\overline{C^0_{La}} + I)$. The source compositions ($\overline{C^0_{La}}$, $\overline{C^0_{La}}/\overline{C^0_b}$) are plotted in Figure 3. r is the correlation coefficient. na = not applicable.

tively. The CR method and the SI method for residual peridotites are illustrated using the orogenic lherzolites from Lanzo as an example. Further work may extend application of the two inversion methods to different kind of residual peridotites (e.g., abyssal peridotites, fore-arc peridotites) or their clinopyroxenes produced in different tectonic settings, provided that the requirements for meaningful inversion of partial melting are satisfied.

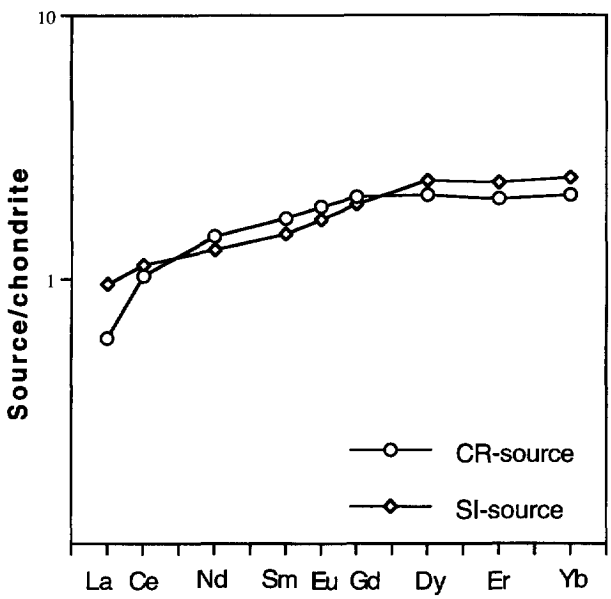

Fig. 4. Comparison of the C1 chondrite-normalized source compositions obtained by the CR method and the SI method, respectively. The $(\overline{C^0_{Ce}})_N$ from the SI method is also estimated as the average value of $(\overline{C^0_{La}})_N$ and $(\overline{C^0_{Nd}})_N$.

Acknowledgments—The comments of Dan McKenzie and an anonymous reviewer significantly improved an earlier version of the manuscript. I am also very grateful to Alan Zindler for his support and to Karl Turekian for his handling of the manuscript.

REFERENCES

Albarède F. (1983) Inversion of batch melting equations and the trace element pattern of the mantle. *J. Geophys. Res.* **88,** 10573–10583.

Albarède F. (1995) *Introduction to Geochemical Modeling.* Cambridge Univ. Press.

Allègre C. J. and Minster J. F. (1978) Quantitative models of trace element behavior in magmatic processes. *Earth Planet. Sci. Lett.* **38,** 1–25.

Anders E. and Ebihara M. (1982) Solar-system abundances of the elements. *Geochim. Cosmochim. Acta* **46,** 2363–2380.

Cebriá J. M. and López-Ruiz J. (1996) A refined method for trace element modeling of nonmodal batch partial melting processes: The Cenozoic continental volcanism of Calatrava, central Spain. *Geochim. Cosmochim. Acta* **60,** 1355–1366.

Frey F. A. (1984) Rare earth element abundances in the upper mantle rocks. In *Rare Earth Element Geochemistry* (ed. P. Henderson), pp. 153–203. Elsevier.

Frey F. A., Green D. F., and Roy S. D. (1978) Integrated models of basalt petrogenesis: A study of quartz tholeiites melilitites from southeastern Australia utilizing geochemical and experimental petrological data. *J. Petrol.* **19,** 463–513.

Frey F. A., Suen C. Y., and Stockman H. W. (1985) The Ronda high temperature peridotite: Geochemistry and petrogenesis. *Geochim. Cosmochim. Acta* **49,** 2469–2491.

Hartmann G. and Wedepohl K. H. (1993) The composition of peridotites from the Ivrea Complex, northern Italy: Residues from melt extraction. *Geochim. Cosmochim. Acta* **57,** 1761–1782.

Hofmann A. W. and Feigenson M. D. (1983) Case studies on the origin of basalt: I. Theory and reassessment of Grenada basalts. *Contrib. Mineral. Petrol.* **84,** 382–389.

Jagoutz E. et al. (1979) The abundances of major, minor, and trace elements in the earth's mantle as derived from primitive ultramafic nodules. *Proc. Lunar Planet. Sci. Conf. 10th,* 2031–2050.

Johnson K.T.M., Dick H. J. B., and Shimizu N. (1990) Melting in the oceanic mantle: An ion microprobe study of diopside in abyssal peridotite. *J. Geophys. Res.* **95,** 2661–2678.

Kempton P. D. (1985) Mineralogical and geochemical evidence for

differing styles of metasomatism in spinel lherzolite xenoliths: Enriched mantle source regions of basalts? In *Mantle Metasomatism* (ed. M. A. Menzies and C. J. Hawkesworth), pp. 45–89. Academic press.

Langmuir C. H., Bender J. F., Bence A. E., Hanson G. N., and Taylor S. R. (1977) Petrogenesis of basalts from the FAMOUS area, Mid-Atlantic ridge. *Earth Planet. Sci. Lett.* **36,** 133–156.

Loubet M. and Allègre C. J. (1982) Trace elements in orogenic lherzolites reveal the complex history of the upper mantle. *Nature* **298,** 809–814.

Loubet M., Shimizu N., and Allègre C. J. (1975) Rare earth elements in Alpine peridotites. *Contrib. Mineral. Petrol.* **53,** 1–12.

Maaløe S. (1994) Estimation of the degree of partial melting using concentration ratios. *Geochim. Cosmochim. Acta* **58,** 2519–2525.

Maaløe S. (1996) Geochemical aspects of primary magma accumulation from extended source regions. *Geochim. Cosmochim. Acta* **59,** 5091–5101.

Maaløe S. and Aoki K. (1977) The major element composition of the upper mantle estimated from the composition of lherzolites. *Contrib. Mineral. Petrol.* **63,** 161–173.

Maaløe S. and Johnson A. D. (1986) Geochemical aspects of some accumulation models for primary magmas. *Contrib. Mineral. Petrol.* **93,** 449–458.

McKenzie D. (1985a) ^{230}Th-^{238}U disequilibrium and the melting processes beneath ridge axes. *Earth Planet. Sci. Lett.* **72,** 149–157.

McKenzie D. (1985b) The extraction of magma from the crust and mantle. *Earth Planet. Sci. Lett.* **74,** 81–91.

McKenzie D. and O'Nions R. K. (1991) Partial melt distributions from inversion of rare earth element concentrations. *J. Petrology* **32,** 1021–1091.

Menzies M., Rodeers N., Tindle A., and Hawkesworth C. (1985) Metasomatic and enrichment processes in lithospheric peridotites, an effect of asthenosphere-lithosphere interaction. In *Mantle Metasomatism* (ed. M. Menzies and C. J. Hawkesworth), pp. 313–363. Academic Press.

Minster J. F. and Allègre C. J. (1978) Systematic use of trace elements in igneous processes, part III: Inverse problem of partial melting in volcanic suites. *Contrib. Mineral. Petrol.* **68,** 37–52.

O'Hara M. J. (1985) Importance of the shape of the melting regime during partial melting of the mantle. *Nature* **314,** 58–62.

Ottonello G., Piccardo G. B., and Hamilton P. J. (1979) Petrogenesis of some Ligurian peridotites., II. Rare earth element chemistry. *Geochim. Cosmochim. Acta* **43,** 1273–1284.

Plank T. and Langmuir C. L. (1992) Effects of the melting regime on the compositions of the oceanic crust. *J. Geophys. Res.* **97,** 19749–19770.

Prinzhofer A. and Allègre C. J. (1985) Residual peridotites and the mechanisms of partial melting. *Earth Planet. Sci. Lett.* **74,** 251–265.

Qin Z. (1993) Dynamics of melt generation beneath mid-ocean ridge axes: Theoretical analysis based on ^{238}U-^{230}Th-^{226}Ra and ^{235}U-^{231}Pa disequilibria. *Geochim. Cosmochim. Acta* **57,** 1629–1634.

Ringwood A. E. (1975) *Composition and Petrology of the Earth's Mantle*. McGraw-Hill.

Shaw D. M. (1970) Trace element fractionation during anatexis. *Geochim. Cosmochim. Acta* **34,** 237–243.

Sims K. W. W. and DePaolo D. J. (1997) Inferences about mantle magma sources from incompatible element concentration ratios in oceanic basalts. *Geochim. Cosmochim. Acta* **61,** 765–784.

Sun S. S. (1982) Geochemical composition and origin of the earth's primitive mantle. *Geochim. Cosmochim. Acta* **46,** 179–192.

Taylor S. R. and McLennan S. M. (1985) *The Continental Crust: Its Composition and Evolution*. Blackwell.

Treuil M. and Joron J. L. (1975) Utilisation des èlèments hygromamatophiles pour la simplification de la modelisation quantitative des processes magmatiques. Examples des L'Afar et de la Dorsale Mèdioatlantique. *Soc. Ital. Mineral. Petrol.* **31,** 125–1174.

Wedepohl K. H. (1991) Chemical composition and fractionation of the continental crust. *Geol. Rundsch.* **80,** 207–223.

Wilshire H. G. (1984) Mantle metasomatism: The REE story. *Geology* **12,** 395–398.

Zindler A. and Hart S. R. (1986) Chemical geodynamics. *Ann. Rev. Earth Planet. Sci.* **14,** 493–571.

Zindler A., Staudigel H., Hart S. R., Enders R., and Goldstein S. (1983) Neodymium and strontium isotopic study of a mafic layer from Ronda ultramafic complex. *Nature* **304,** 226–230.

Zou H. and Zindler A. (1996) Constraints on the degree of dynamic partial melting and source composition using concentration ratios in magmas. *Geochim. Cosmochim. Acta*. **60,** 711–717.

APPENDIX

List of Symbols

C_r	concentration in residues
C_{ra}	concentration of a highly incompatible element in residual peridotites
C_{rb}	concentration of a less incompatible element in residual peridotites
C^0	the source concentration
C^{cpx}	concentration of a trace element in residual clinopyroxene
C_a^{cpx}	concentration of a highly incompatible element in residual clinopyroxene
C_b^{cpx}	concentration of a less incompatible element in residual clinopyroxene
$C^{0,cpx}$	initial source concentration in clinopyroxene
R_a	concentration ratio for a highly incompatible element
R_b	concentration ratio for a less incompatible element
Q	$= R^{P/(1-P)}$ for inversion of non-modal fractional melting using clinopyroxene in Table 2
D^{cpx}	clinopyroxene/melt distribution coefficient
D	bulk distribution coefficient
D^0	initial bulk distribution coefficient
D_a^0	initial bulk distribution coefficient for a highly incompatible element
D_b^0	initial bulk distribution coefficient for a less incompatible element
P	bulk distribution coefficient of an element for the minerals entering into the liquid
$\overline{C_{La}^0}$	the average value of calculated source La concentrations using the SI method
$\bar{f}$	the average value of calculated partial melting degrees using the CR method
f	the degree of partial melting
X	the mass fraction of liquid extracted
ϕ	volume porosity of the residual solid
ρ_f	the density of melt
ρ_s	the density of solid matrix
S	slope
I	intercept